16

Boundary-layer flows with algebraic property

In most cases the velocity profiles and temperature of boundary layer flows decay exponentially. However, as reported by Kuiken [110, 111], solutions of some boundary layer flows behave algebraically at infinity.

For instance Kuiken [111] analyzed a glass-fiber production process and obtained, by means of various similarity transformations, a set of two coupled nonlinear differential equations

$$f'''(\eta) + \theta(\eta) - f'^2(\eta) = 0, \tag{16.1}$$

$$\theta''(\eta) = 3\,\sigma\, f'(\eta)\,\theta(\eta), \tag{16.2}$$

subject to the boundary conditions

$$f(0) = f'(0) = 0, \theta(0) = 1, \tag{16.3}$$

$$f'(+\infty) = \theta(+\infty) = 0, \tag{16.4}$$

where the prime denotes differentiation with respect to the similarity variable η, σ is the Prandtl number, $f(\eta)$ and $\theta(\eta)$ relate to the velocity profile and temperature distribution of the boundary layer, respectively. For details, the reader is referred to Kuiken [111].

Kuiken [111] presented a solution that contains a parameter that had to be determined by numerical methods. Kuiken's solution [111] is fundamentally analytic-numerical. To the best of the author's knowledge, no one has reported an explicit, fully analytic solution of the coupled nonlinear equations (16.1) and (16.2). In this chapter the homotopy analysis method is employed to yield this type of solution.

16.1 Homotopy analysis solution

16.1.1 Asymptotic property

From (16.4), both $f'(\eta)$ and $\theta(\eta)$ tend to zero as $\eta \to +\infty$. So, it is important to know the behavior of the solution at infinity. As pointed out by Kuiken [111], both $f(\eta)$ and $\theta(\eta)$ decay algebraically as $\eta \to +\infty$.

Under the transformation

$$\xi = 1 + \lambda\,\eta, \qquad F(\xi) = f'(\eta), \qquad S(\xi) = \theta(\eta), \tag{16.5}$$

where $\lambda > 0$ is the so-called spatial-scale parameter, Equations (16.1) and (16.2) become

$$\lambda^2\, F''(\xi) + S(\xi) - F^2(\xi) = 0, \tag{16.6}$$

$$\lambda^2\, S''(\xi) = 3\,\sigma\, F(\xi)\, S(\xi), \tag{16.7}$$

subject to the boundary conditions

$$F(1) = 0, S(1) = 1, \tag{16.8}$$

$$F(+\infty) = S(+\infty) = 0. \tag{16.9}$$

Define

$$F \sim \xi^{\alpha_1}, \qquad S \sim \xi^{\alpha_2} \tag{16.10}$$

as the asymptotic expressions of $F(\xi)$ and $S(\xi)$ as $\xi \to +\infty$. Substituting them into Equations (16.6) and (16.7) and balancing the main terms of each equation, we have

$$\alpha_1 = -2, \qquad \alpha_2 = -4. \tag{16.11}$$

Thus, considering their algebraic property at infinity, $F(\xi)$ and $S(\xi)$ can be expressed by the base functions

$$\left\{\xi^{-n} \mid n \geq 2\right\} \tag{16.12}$$

in the forms:

$$F(\xi) = \sum_{n=2}^{+\infty} \frac{a_n}{\xi^n}, \tag{16.13}$$

$$S(\xi) = \sum_{n=4}^{+\infty} \frac{b_n}{\xi^n}, \tag{16.14}$$

respectively, where a_n, b_n are coefficients. The above expressions provide the so-called *rules of solution expression* of $F(\xi)$ and $S(\xi)$, respectively.

16.1.2 Zero-order deformation equation

Under the *rules of solution expression* denoted by (16.13) and (16.14) and from Equations (16.8) and (16.9), it is easy to choose

$$F_0(\xi) = \gamma\left(\xi^{-2} - \xi^{-3}\right), \qquad S_0(\xi) = \xi^{-4} \tag{16.15}$$

as the initial guesses of $F(\xi)$ and $S(\xi)$, respectively, where γ is an auxiliary parameter. Furthermore, under the *rules of solution expression* denoted by

(16.13) and (16.14) and from Equations (16.6) and (16.7), we select the auxiliary linear operators

$$\mathcal{L}_F\Phi = \left(\frac{\xi}{3}\right)\frac{\partial^2\Phi}{\partial\xi^2} + \frac{\partial\Phi}{\partial\xi}, \tag{16.16}$$

$$\mathcal{L}_S\Phi = \left(\frac{\xi}{5}\right)\frac{\partial^2\Phi}{\partial\xi^2} + \frac{\partial\Phi}{\partial\xi} \tag{16.17}$$

with the properties

$$\mathcal{L}_F\left(C_1 + C_2\,\xi^{-2}\right) = 0, \tag{16.18}$$

$$\mathcal{L}_S\left(C_3 + C_4\,\xi^{-4}\right) = 0, \tag{16.19}$$

where C_1, C_2, C_3, and C_4 are coefficients. For simplicity, from Equations (16.6) and (16.7), we define the nonlinear operators

$$\mathcal{N}_F\left[\Phi(\xi;q), \Theta(\xi;q)\right] = \lambda^2\,\frac{\partial\Phi(\xi;q)}{\partial\xi^2} + \Theta(\xi;q) - \Phi^2(\xi;q), \tag{16.20}$$

$$\mathcal{N}_S\left[\Phi(\xi;q), \Theta(\xi;q)\right] = \lambda^2\,\frac{\partial^2\Theta(\xi;q)}{\partial\xi^2} - 3\,\sigma\,\Phi(\xi;q)\,\Theta(\xi;q), \tag{16.21}$$

where $q \in [0,1]$ is an embedding parameter, $\Phi(\xi;q)$ and $\Theta(\xi;q)$ are real functions of ξ and q. Let $\hbar_F$ and $\hbar_S$ denote the nonzero auxiliary parameters, $H_F(\xi)$ and $H_S(\xi)$ the nonzero auxiliary functions, respectively. We construct the zero-order deformation equations

$$\begin{aligned}&(1-q)\,\mathcal{L}_F\left[\Phi(\xi;q) - F_0(\xi)\right]\\ &= q\,\hbar_F\,H_F(\xi)\,\mathcal{N}_F\left[\Phi(\xi;q), \Theta(\xi;q)\right],\end{aligned} \tag{16.22}$$

$$\begin{aligned}&(1-q)\,\mathcal{L}_S\left[\Theta(\xi;q) - S_0(\xi)\right]\\ &= q\,\hbar_S\,H_S(\xi)\,\mathcal{N}_S\left[\Phi(\xi;q), \Theta(\xi;q)\right],\end{aligned} \tag{16.23}$$

subject to the boundary conditions

$$\Phi(1;q) = \Phi(+\infty;q) = \Theta(+\infty;q) = 0, \quad \Theta(1;q) = 1, \tag{16.24}$$

where $q \in [0,1]$ is the embedding parameter.

When $q = 0$, it is easy to demonstrate that

$$\Phi(\xi;0) = F_0(\xi),\ \Theta(\xi;0) = S_0(\xi), \tag{16.25}$$

where $F_0(\xi)$ and $S_0(\xi)$ are the initial guesses defined by (16.15). When $q = 1$, since

$$\hbar_F \neq 0,\ \ \hbar_S \neq 0,\ \ H_F(\xi) \neq 0,\ \ H_S(\xi) \neq 0,$$

the zero-order deformation equations (16.22) to (16.24) are equivalent to the original equations (16.6) to (16.9), provided

$$\Phi(\xi;1) = F(\xi),\ \Theta(\xi;1) = S(\xi). \tag{16.26}$$

Thus, as q increases from 0 to 1, $\Phi(\xi;q)$ and $\Theta(\xi;q)$ vary (or deform) from the initial guesses $F_0(\xi), S_0(\xi)$ to the solutions $F(\xi), S(\xi)$ of Equations (16.6) to (16.9), respectively.

By Taylor's theorem and using (16.25), we obtain the power series

$$\Phi(\xi;q) = F_0(\xi) + \sum_{n=1}^{+\infty} F_n(\xi)\, q^n, \tag{16.27}$$

$$\Theta(\xi;q) = S_0(\xi) + \sum_{n=1}^{+\infty} S_n(\xi)\, q^n, \tag{16.28}$$

where

$$F_n(\xi) = \frac{1}{n!}\frac{\partial^n \Phi(\xi;q)}{\partial q^n}\bigg|_{q=0}, \qquad S_n(\xi) = \frac{1}{n!}\frac{\partial^n \Theta(\xi;q)}{\partial q^n}\bigg|_{q=0}. \tag{16.29}$$

Assuming that the spatial-scale parameter λ, the auxiliary parameter γ in (16.15), the auxiliary parameters $\hbar_F, \hbar_S$ and the auxiliary functions $H_F(\xi)$, $H_S(\xi)$ are properly chosen so that the above series converge at $q = 1$, we have, using (16.26),

$$F(\xi) = F_0(\xi) + \sum_{n=1}^{+\infty} F_n(\xi), \tag{16.30}$$

$$S(\xi) = S_0(\xi) + \sum_{n=1}^{+\infty} S_n(\xi). \tag{16.31}$$

The corresponding mth-order approximations are given by

$$F(\xi) \approx F_0(\xi) + \sum_{n=1}^{m} F_n(\xi), \tag{16.32}$$

$$S(\xi) \approx S_0(\xi) + \sum_{n=1}^{m} S_n(\xi). \tag{16.33}$$

16.1.3 High-order deformation equation

For conciseness, define the vectors

$$\vec{F}_m = \{F_0(\xi), F_1(\xi), F_2(\xi), \cdots, F_m(\xi)\}$$

and

$$\vec{S}_m = \{S_0(\xi), S_1(\xi), S_2(\xi), \cdots, S_m(\xi)\}\,.$$

Differentiating the zero-order deformation equations (16.22) to (16.24) n times with respective to q, then dividing by $n!$, and finally setting $q = 0$, we have the high-order deformation equations

$$\mathcal{L}_F\left[F_n(\xi) - \chi_n F_{n-1}(\xi)\right] = \hbar_F\, H_F(\xi)\, R_n^F(\vec{F}_{n-1}, \vec{S}_{n-1}), \tag{16.34}$$

$$\mathcal{L}_S\left[S_n(\xi) - \chi_n S_{n-1}(\xi)\right] = \hbar_S\, H_S(\xi)\, R_n^S(\vec{F}_{n-1}, \vec{S}_{n-1}), \tag{16.35}$$

subject to the boundary conditions

$$F_n(1) = S_n(1) = F_n(+\infty) = S_n(+\infty) = 0, \tag{16.36}$$

where χ_n is defined by (2.42) and

$$R_n^F(\vec{F}_{n-1}, \vec{S}_{n-1}) = \lambda^2\, F_{n-1}''(\xi) + S_{n-1}(\xi) - \sum_{j=0}^{n-1} F_j(\xi)\, F_{n-1-j}(\xi), \tag{16.37}$$

$$R_n^S(\vec{F}_{n-1}, \vec{S}_{n-1}) = \lambda^2\, S_{n-1}''(\xi) - 3\,\sigma \sum_{j=0}^{n-1} F_j(\xi)\, S_{n-1-j}(\xi). \tag{16.38}$$

Note that the high-order deformation equations (16.34) to (16.36) are uncoupled and linear. It is therefore easy to solve them, using symbolic computation software.

Under the *rules of the solution expression* denoted by (16.13) and (16.14) and from Equations (16.34) and (16.35), the auxiliary functions $H_F(\xi)$ and $H_S(\xi)$ may be written as

$$H_F(\xi) = \xi^{\kappa_1},\ H_S(\xi) = \xi^{\kappa_2}, \tag{16.39}$$

where κ_1 and κ_2 are integers. It is found that, when $\kappa_1 \geq 1$ and/or $\kappa_2 \geq 1$, the term $\ln \xi$ appears in the solution expressions, which does not conform to the *rules of solution expression* denoted by (16.13) and (16.14). When $\kappa_1 \leq -1$ and/or $\kappa_2 \leq -1$, $F(\xi)$ and $S(\xi)$ do not contain the terms ξ^{-2} and ξ^{-4}, respectively. This is not in accordance with the *rule of coefficient ergodicity*. To adhere to both the *rules of solution expression* and the *rule of coefficient ergodicity*, we must choose

$$\kappa_1 = \kappa_2 = 0,$$

corresponding to

$$H_F(\xi) = H_S(\xi) = 1. \tag{16.40}$$

Now, the inhomogeneous terms of Equations (16.34) and (16.35) are completely known.

16.1.4 Recursive formulations

By solving the first several high-order deformation equations (16.34) to (16.36), $F_n(\xi)$ and $S_n(\xi)$ can be expressed by

$$F_n(\xi) = \xi^{-2} \sum_{j=0}^{2n+1} a_{n,j}\, \xi^{-j}, \qquad S_n(\xi) = \xi^{-4} \sum_{j=0}^{2n} b_{n,j}\, \xi^{-j}, \quad (16.41)$$

where $a_{n,j}$ and $b_{n,j}$ are coefficients. Substituting them into Equations (16.34) to (16.36), we have the recursive formulae ($j \geq 1$)

$$\begin{aligned} a_{n,j} &= \chi_n\, \chi_{2n+1-j}\, a_{n-1,j} \\ &+ \frac{3\, \hbar_F \left[\chi_{2n+2-j}\, \lambda^2\, (j+1)(j+2) a_{n-1,j-1} + \chi_{2n+1-j} b_{n-1,j-1} - A_{n,j-1}\right]}{j(j+2)}, \end{aligned} \quad (16.42)$$

$$\begin{aligned} b_{n,j} &= \chi_n\, \chi_{2n-j}\, b_{n-1,j} \\ &+ \frac{5\, \hbar_S \left[\chi_{2n+1-j}\, \lambda^2\, (j+3)(j+4) b_{n-1,j-1} - 3\sigma\, B_{n,j-1}\right]}{j(j+4)}, \end{aligned} \quad (16.43)$$

and

$$a_{n,0} = -\sum_{j=1}^{2n+1} a_{n,j}, \qquad b_{n,0} = -\sum_{j=1}^{2n} b_{n,j}, \quad (16.44)$$

where

$$A_{n,i} = \sum_{j=0}^{n-1} \sum_{r=\max\{0,i+2j-2n+1\}}^{\min\{2j+1,i\}} a_{j,r}\, a_{n-j-1,i-r}, \quad (16.45)$$

$$B_{n,i} = \sum_{j=0}^{n-1} \sum_{r=\max\{0,i+2j-2n+2\}}^{\min\{2j+1,i\}} a_{j,r}\, b_{n-j-1,i-r}. \quad (16.46)$$

Using (16.15), we have the first three coefficients

$$a_{0,0} = \gamma,\ a_{0,1} = -\gamma,\ b_{0,0} = 1. \quad (16.47)$$

From these and using the above recursive formulae, we can calculate all other coefficients $a_{n,j}$ and $b_{n,j}$, successively. Thus, we have the explicit analytic solutions

$$F(\xi) = \sum_{n=0}^{+\infty} \sum_{j=0}^{2n+1} \frac{a_{n,j}}{\xi^{j+2}}, \qquad S(\xi) = \sum_{n=0}^{+\infty} \sum_{j=0}^{2n} \frac{b_{n,j}}{\xi^{j+4}}. \quad (16.48)$$

Using the transformation (16.5) we obtain

$$f'(\eta) = \sum_{n=0}^{+\infty} \sum_{j=0}^{2n+1} \frac{a_{n,j}}{(1+\lambda\,\eta)^{j+2}}, \quad \theta(\eta) = \sum_{n=0}^{+\infty} \sum_{j=0}^{2n} \frac{b_{n,j}}{(1+\lambda\,\eta)^{j+4}}. \tag{16.49}$$

The mth-order approximations are

$$f'(\eta) \approx \sum_{n=0}^{m} \sum_{j=0}^{2n+1} \frac{a_{n,j}}{(1+\lambda\,\eta)^{j+2}}, \quad \theta(\eta) \approx \sum_{n=0}^{m} \sum_{j=0}^{2n} \frac{b_{n,j}}{(1+\lambda\,\eta)^{j+4}}, \tag{16.50}$$

which give

$$f(\eta) \approx \sum_{n=0}^{m} \sum_{j=0}^{2n+1} \frac{a_{n,j}}{\lambda\,(j+1)} \left[1 - \frac{1}{(1+\lambda\,\eta)^{j+1}}\right] \tag{16.51}$$

and

$$f''(0) \approx -\lambda \sum_{n=0}^{m} \sum_{j=0}^{2n+1} (j+2) a_{n,j}, \tag{16.52}$$

$$f(+\infty) \approx \sum_{n=0}^{m} \sum_{j=0}^{2n+1} \frac{a_{n,j}}{\lambda\,(j+1)}, \tag{16.53}$$

$$\theta'(0) \approx -\lambda \sum_{n=0}^{m} \sum_{j=0}^{2n} (j+4) b_{n,j}. \tag{16.54}$$

16.1.5 Convergence theorem

THEOREM 16.1

If the solution series (16.30) and (16.31) are convergent, where $F_n(\xi)$ and $S_n(\xi)$ are governed by Equations (16.34) to (16.36) under the definitions (16.37) to (16.38), and (2.42), they must be the solution of Equations (16.6) to (16.9)

Proof: If the solution series (16.30) and (16.31) are convergent, it is necessary that

$$\lim_{m\to+\infty} F_m(\xi) = 0, \qquad \lim_{m\to+\infty} S_m(\xi) = 0.$$

Then, from (16.16) and (16.17),

$$\mathcal{L}_F\left[\lim_{m\to+\infty} F_m(\xi)\right] = 0, \qquad \mathcal{L}_S\left[\lim_{m\to+\infty} S_m(\xi)\right] = 0.$$

From Equations (16.34) and (16.35), we have, using (2.42),

$$\hbar_F\, H_F(\xi) \sum_{n=1}^{m} R_n^F(\vec{F}_{n-1}, \vec{S}_{n-1}) = \mathcal{L}_F\left[F_m(\xi)\right]$$

and

$$\hbar_S \, H_S(\xi) \, \sum_{n=1}^{m} R_n^S(\vec{F}_{n-1}, \vec{S}_{n-1}) = \mathcal{L}_S \left[S_m(\xi) \right].$$

Therefore,

$$\hbar_F \, H_F(\xi) \, \sum_{n=1}^{+\infty} R_n^F(\vec{F}_{n-1}, \vec{S}_{n-1}) = \mathcal{L}_F \left[\lim_{m \to +\infty} F_m(\xi) \right] = 0$$

and

$$\hbar_S \, H_S(\xi) \, \sum_{n=1}^{+\infty} R_n^S(\vec{F}_{n-1}, \vec{S}_{n-1}) = \mathcal{L}_S \left[\lim_{m \to +\infty} S_m(\xi) \right] = 0,$$

which give, since $\hbar_F \neq 0, \hbar_S \neq 0, H_F(\xi) \neq 0$ and $H_S(\xi) \neq 0$,

$$\sum_{n=1}^{+\infty} R_n^F(\vec{F}_{n-1}, \vec{S}_{n-1}) = 0$$

and

$$\sum_{n=1}^{+\infty} R_n^S(\vec{F}_{n-1}, \vec{S}_{n-1}) = 0.$$

Substituting (16.37) and (16.38) into above two expressions and simplifying them, we obtain

$$\lambda^2 \, \frac{\partial^2}{\partial \xi^2} \left[\sum_{n=0}^{+\infty} F_n(\xi) \right] + \sum_{n=0}^{+\infty} S_n(\xi) - \left[\sum_{n=0}^{+\infty} F_n(\xi) \right]^2 = 0 \qquad (16.55)$$

and

$$\lambda^2 \, \frac{\partial^2}{\partial \xi^2} \left[\sum_{n=0}^{+\infty} S_n(\xi) \right] - 3 \, \sigma \, \left[\sum_{n=0}^{+\infty} F_n(\xi) \right] \left[\sum_{n=0}^{+\infty} S_n(\xi) \right] = 0. \qquad (16.56)$$

From (16.15) and (16.36), we obviously have

$$\sum_{n=0}^{+\infty} F_n(1) = \sum_{n=0}^{+\infty} F_n(+\infty) = \sum_{n=0}^{+\infty} S_n(+\infty) = 0, \quad \sum_{n=0}^{+\infty} S_n(1) = 1. \qquad (16.57)$$

Comparing Equations (16.55) to (16.57) with Equations (16.6) to (16.9), it is clear that the convergent series (16.30) and (16.31) are the solutions of the two coupled nonlinear differential equations. This ends the proof.

16.2 Result analysis

There exist four auxiliary parameters: $\hbar_F, \hbar_S, \lambda$, and γ. We have therefore a four-parameter family of solution expressions. According to Theorem 16.1, we need only to focus on the choice of the four auxiliary parameters to ensure that the solution series (16.30) and (16.31) converge.

Note that the initial guess $F_0(\xi)$ defined by (16.15) contains the auxiliary parameter γ. Substituting the initial approximations (16.15) into Equations (16.6) and (16.7) and balancing the main terms, we obtain a set of two algebraic equations of λ and γ, which give

$$\lambda = \sqrt{\frac{3\sigma}{20}}\left(1 - \frac{9\sigma}{10}\right)^{-1/4}, \qquad \gamma = \left(1 - \frac{9\sigma}{10}\right)^{-1/2}. \tag{16.58}$$

Although the above expressions are valid only when $\sigma < 10/9$, it provides valuable information for the choice of λ and γ. From (16.58), it is obvious that

$$\gamma \sim 1, \qquad \lambda \sim \sqrt{\sigma}$$

for $\sigma \ll 1$.

In general, for any given Prandtl number σ, we can investigate the influence of the four auxiliary parameters $\lambda, \gamma, \hbar_F$, and $\hbar_S$ on the convergence of solution series and then choose a set of proper values. For example, let us consider the case $\sigma = 1$. Note that

$$f''(0) = \lambda\, F'(0), \qquad \theta'(0) = \lambda\, S'(0)$$

are related with the skin friction and thermal flux and therefore have important physical meaning. For simplicity, we first study the influence of the four auxiliary parameters on the convergence of $f''(0)$ and $\theta'(0)$. When $\hbar_F = \hbar_S = -1/2$ and $\gamma = 1, 2, 3$, both $\theta'(0)$ and $f''(0)$ are convergent in a region of λ that becomes the largest when $\gamma = 3$, as shown in Figures 16.1 and 16.2. From these two figures, it is clear that the series of $f''(0)$ and $\theta'(0)$ converge if $\lambda = 1/3, \gamma = 3$, and $\hbar_F = \hbar_S = -1/2$. To ensure this, we can further investigate the influence of the auxiliary parameters $\hbar_F$ and $\hbar_S$ on the convergence of solution series when $\lambda = 1/3, \gamma = 3$, and $\hbar_F = \hbar_S = \hbar$ by plotting the so-called $\hbar$-curves (see page 26 and §3.5.1) of $f''(0)$ and $\theta'(0)$, as shown in Figure 16.3. When $\sigma = 1$, the series of $f''(0)$ and $\theta'(0)$ converge by means of $\lambda = 1/3, \gamma = 3$, and $\hbar_F = \hbar_S = -1/2$, as shown in Table 16.1. Generally, for given Prandtl number σ, we can choose the auxiliary parameters $\lambda, \gamma, \hbar_F$, and $\hbar_S$ in the similar way to ensure that the series of $f''(0)$ and $\theta'(0)$ converge. For example, the series of $f''(0)$ and $\theta'(0)$ converge when $\sigma = 1/10$ by means of $\lambda = 1/5, \gamma = 1$, and $\hbar_F = \hbar_S = -1/2$, and when $\sigma = 10$ by $\lambda = 1/3, \gamma = 1, \hbar_F = -1/4$, and $\hbar_S = -1/10$, respectively. The solution series

converge when $\sigma > 10$ by means of $\lambda = 1, \gamma = 1, \hbar_F = -1/4$, and $\hbar_S = -1/\sigma$, and when $\sigma < 1/10$ by means of $\gamma = 1, \hbar_F = \hbar_S = -1/2$, and $\lambda = 1/5$ or even smaller. Furthermore, as long as the series of $f''(0)$ and $\theta'(0)$ are convergent, the corresponding solution series of $f(\xi)$ and $\theta(\xi)$ also converge in the whole region $0 \leq \xi < +\infty$, as shown in Figures 16.4 and 16.5.

The convergence of the series of $f''(0)$ and $\theta'(0)$ can be accelerated using the homotopy-Padé technique (see page 38 and §3.5.2), as shown in Tables 16.2 and 16.3. When $\hbar_F = \hbar_S = \hbar$, the $[m, m]$ homotopy-Padé approximants do not depend upon $\hbar$.

Note that we obtain an explicit, purely analytic solution of the two coupled nonlinear equations (16.1) and (16.2) by means of the recursive formulae (16.42) to (16.47). The analytic solutions behave algebraically at infinity. In Chapter 15 the homotopy analysis method is successfully applied to solve the Falkner-Skan boundary layer flows that behave exponentially at infinity. The homotopy analysis method is therefore valid for these two different types of boundary layer flows.

TABLE 16.1
The mth-order approximations of $f''(0)$ and $\theta'(0)$ when $\sigma = 1$ by means of $\lambda = 1/3, \gamma = 3$, and $\hbar_F = \hbar_S = -1/2$ compared with Kuiken's result [111].

m	$f''(0)$	$\theta'(0)$
5	0.713814	-0.831716
10	0.706453	-0.765271
15	0.702547	-0.769478
20	0.697170	-0.771491
25	0.694380	-0.770640
30	0.693538	-0.770001
35	0.693342	-0.769872
40	0.693268	-0.769879
45	0.693227	-0.769876
50	0.693213	-0.769866
Kuiken's result	0.693212	-0.769861

TABLE 16.2
The $[m, m]$ homotopy-Padé approximations of $f''(0)$ compared with Kuiken's result [111].

$[m, m]$	$\sigma = 1/10$ $\lambda = 1/5, \gamma = 1$	$\sigma = 1$ $\lambda = 1/3, \gamma = 3$	$\sigma = 10$ $\lambda = 1/3, \gamma = 1$
$[5, 5]$	0.952170	0.705940	0.433555
$[10, 10]$	0.921936	0.693438	0.452229
$[15, 15]$	0.924108	0.693214	0.447038
$[20, 20]$	0.924087	0.693212	0.447107
$[25, 25]$	0.924088	0.693212	0.447117
$[30, 30]$	0.924086	0.693212	0.447117
$[35, 35]$	0.924084	0.693212	0.447117
$[40, 40]$	0.924083	0.693212	0.447117
$[45, 45]$	0.924083	0.693212	0.447117
$[50, 50]$	0.924083	0.693212	0.447117
Kuiken's result	0.924083	0.693212	0.447117

TABLE 16.3
The $[m, m]$ homotopy-Padé approximations of $\theta'(0)$ compared with Kuiken's result [111].

$[m, m]$	$\sigma = 1/10$ $\lambda = 1/5, \gamma = 1$	$\sigma = 1$ $\lambda = 1/3, \gamma = 3$	$\sigma = 10$ $\lambda = 1/3, \gamma = 1$
$[5, 5]$	-0.347058	-0.774151	-1.61583
$[10, 10]$	-0.350119	-0.770018	-1.49263
$[15, 15]$	-0.350027	-0.769866	-1.49733
$[20, 20]$	-0.350058	-0.769861	-1.49708
$[25, 25]$	-0.350058	-0.769861	-1.49710
$[30, 30]$	-0.350059	-0.769861	-1.49710
$[35, 35]$	-0.350059	-0.769861	-1.49710
$[40, 40]$	-0.350059	-0.769861	-1.49710
$[45, 45]$	-0.350059	-0.769861	-1.49710
$[50, 50]$	-0.350059	-0.769861	-1.49710
Kuiken's result	-0.350059	-0.769861	-1.49710

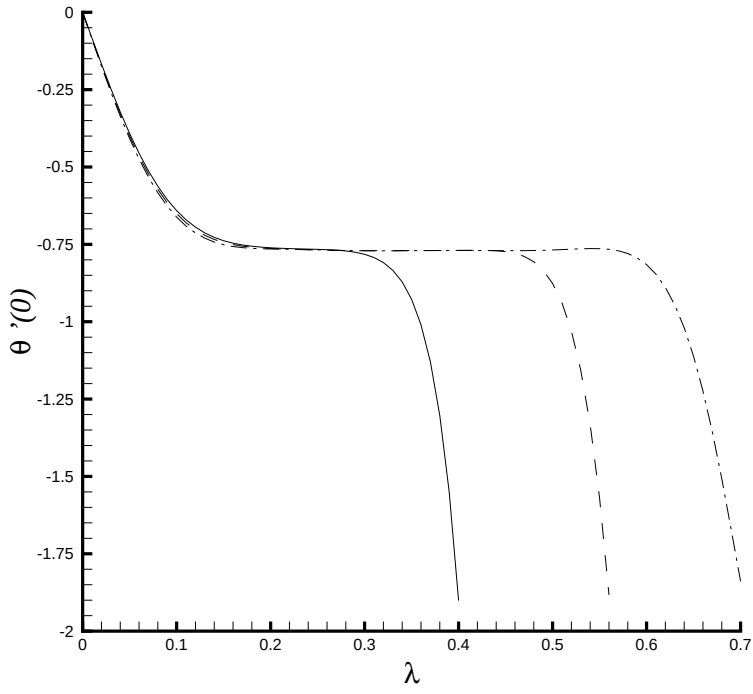

FIGURE 16.1
$\theta'(0)$ versus λ at the 24th order of approximation when $\sigma = 1$ and $\hbar_F = \hbar_S = -1/2$. Solid line: $\gamma = 1$; dashed line: $\gamma = 2$; dash-dotted line: $\gamma = 3$.

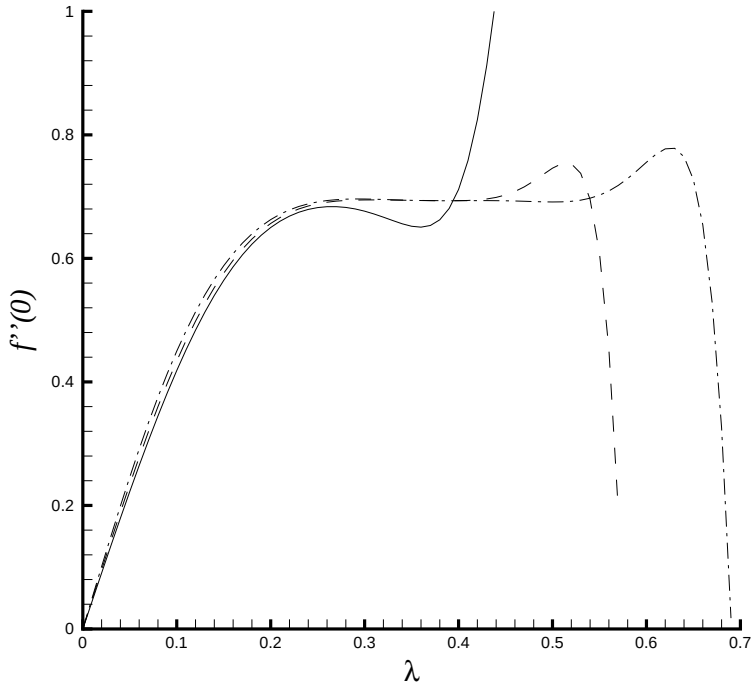

FIGURE 16.2
$f''(0)$ versus λ at the 24th order of approximation when $\sigma = 1$ and $\hbar_F = \hbar_S = -1/2$. Solid line: $\gamma = 1$; dashed line: $\gamma = 2$; dash-dotted line: $\gamma = 3$.

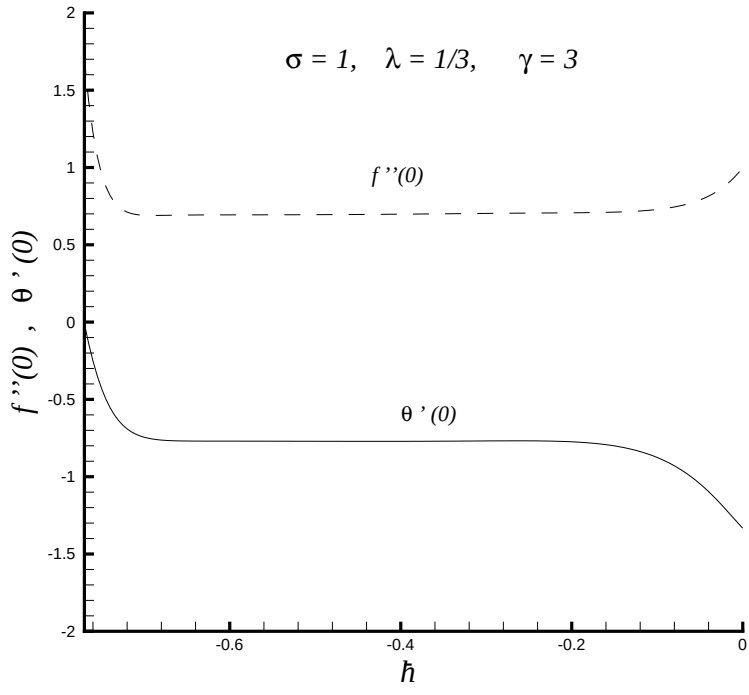

FIGURE 16.3
The $\hbar$-curves of $f''(0)$ and $\theta'(0)$ at the 24th order of approximations when $\sigma = 1$ by means of $\gamma = 3, \lambda = 1/3$, and $\hbar_F = \hbar_S = -1/2$. Solid line: $\theta'(0)$; dashed line: $f''(0)$.

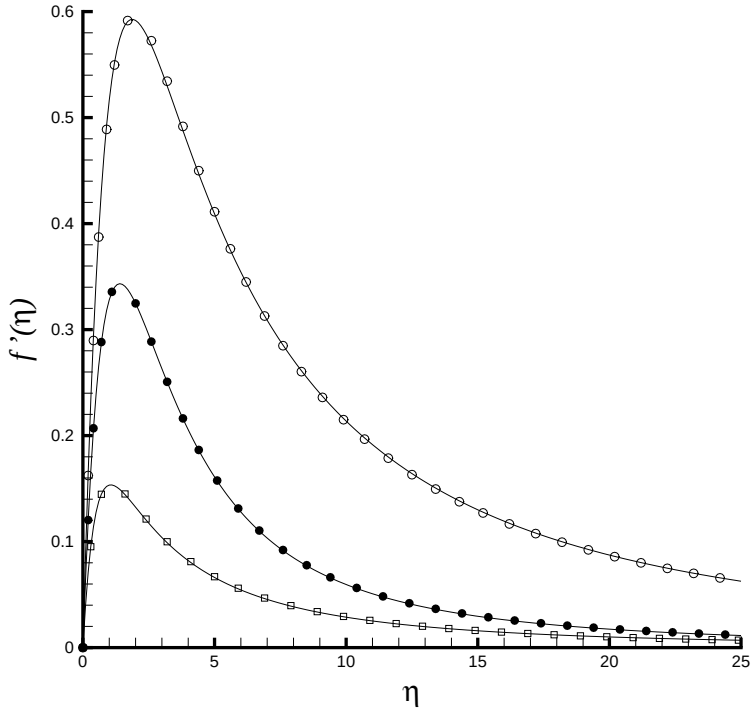

FIGURE 16.4
Comparison of $f'(\eta)$ with numerical results. Open circle: 30th-order approximation when $\sigma = 1/10$ by means of $\hbar_F = \hbar_S = -1/2, \lambda = 1/5$, and $\gamma = 1$; filled-circle: 20th-order approximation when $\sigma = 1$ by means of $\hbar_F = \hbar_S = -1/2, \lambda = 1/3$, and $\gamma = 3$; square: 40th-order approximation when $\sigma = 10$ by means of $\hbar_F = -1/4, \hbar_S = -1/10, \lambda = 1/3$, and $\gamma = 1$; solid lines: numerical results.

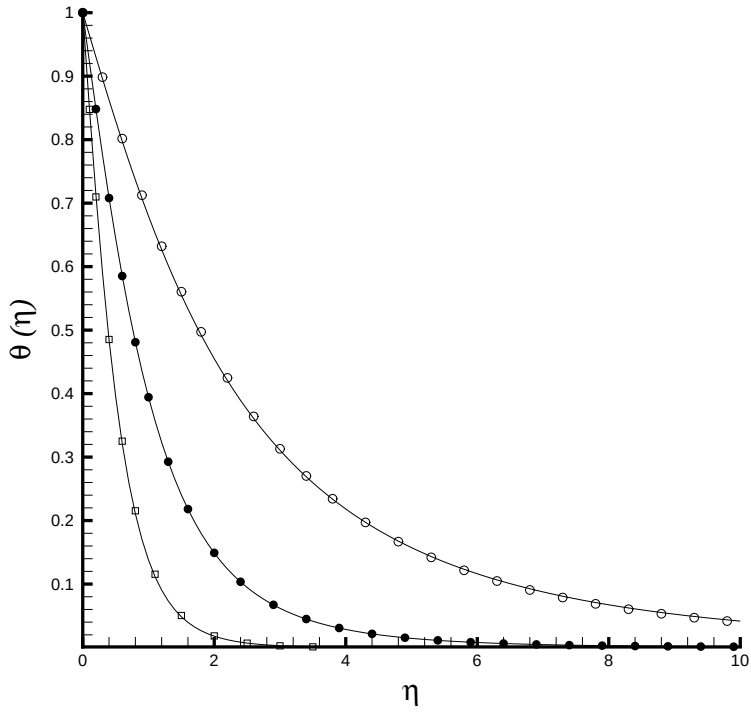

FIGURE 16.5
Comparison of $\theta(\eta)$ with numerical results. Open circle: 20th-order approximation when $\sigma = 1/10$ by means of $\hbar_F = \hbar_S = -1/2, \lambda = 1/5$, and $\gamma = 1$; filled-circle: 20th-order approximation when $\sigma = 1$ by means of $\hbar_F = \hbar_S = -1/2, \lambda = 1/3$, and $\gamma = 3$; square: 20th-order approximation when $\sigma = 10$ by means of $\hbar_F = -1/4, \hbar_S = -1/10, \lambda = 1/3$, and $\gamma = 1$; solid lines: numerical results.